BBA - General Subjects 1862 (2018) 1107–1114

Contents lists available at ScienceDirect

BBA - General Subjects

journal homepage: www.elsevier.com/locate/bbagen

A cooperative transition from the semi-flexible to the flexible regime of polymer elasticity: Mitoxantrone-induced DNA condensation

C.H.M. Lima, G.O. Almeida, M.S. Rocha*

Laboratório de Física Biológica, Departamento de Física, Universidade Federal de Viçosa, Viçosa, Minas Gerais, Brazil

ARTICLE INFO

Keywords:
DNA condensation
Mitoxantrone
Polymer elasticity
Force spectroscopy

ABSTRACT

We report a high cooperative transition from the semi-flexible to the flexible regime of polymer elasticity during the interaction of the DNA molecule with the chemotherapeutic drug Mitoxantrone (MTX). By using single molecule force spectroscopy, we show that the force-extension curves of the DNA-MTX complexes deviate from the typical worm-like chain behavior as the MTX concentration in the sample increases, becoming straight lines for sufficiently high drug concentrations. The behavior of the radius of gyration of the complexes as a function of the bound MTX concentration was used to quantitatively investigate the cooperativity of the condensation process. The present methodology can be promptly applied to other ligands that condense the DNA molecule upon binding, opening new possibilities in the investigation of this type of process and, more generally, in the investigation of phase transitions in polymer physics.

1. Introduction

The interactions of the DNA molecule with ligands such as proteins and drugs is a field important to many areas of knowledge, from the comprehension of basic intracellular processes to the application in medical sciences, especially in cancer chemotherapies. Along the past years, single molecule techniques such as optical and magnetic tweezers, as well as atomic force microscopy, have promoted a major step in the understanding of such interactions [1–6]. In fact, these techniques have opened the possibility of manipulating single DNA-ligand complexes, allowing the determination of force-extension curves (FECs) from which the mechanical properties of the complexes (and the physical chemistry of the interaction [1]) can be extracted. This type of approach is usually known as single molecule force spectroscopy (SMFS).

When using SMFS to study the interactions of the DNA molecule with drugs or proteins, the straightforward approach employed to determine the mechanical parameters of the complexes formed is to fit the experimental FECs to the worm-like chain (WLC) model [7–9]. Nevertheless, such model has its intrinsic limitations, for example, it is valid only for semi-flexible polymers. The bare DNA molecule has a peculiar chemical structure, with two strands forming a double-helix that sets important properties to the biopolymer such as a well-defined negative charge density and a bending stiffness which places DNA in the class of semi-flexible polymers [7,9-11]. When a ligand binds to the double-helix, however, it can change the local bending stiffness as well as the local charge density. Thus, if these changes make the DNA-ligand complex much stiff or soft, the WLC model may fail and the mechanical parameters obtained from the fitting of the FEC are maybe not much realist. Fortunately, a large number of DNA ligands change only slightly the DNA persistence length upon binding. Thus, the complex formed is still a semi-flexible polymer, which justifies the use of the WLC model to analyze the data. Nevertheless, this is not a general property, and there are some ligands that can change drastically the mechanical properties of the DNA molecule upon binding. Maybe the most known examples are ligands that condense the DNA molecule, such as the polyamines spermine and spermidine, and the histone proteins. These cationic ligands considerably reduce the effective persistence length of the complexes formed at low ionic strengths [12,13], facilitating the DNA condensation process. Small drug molecules that induce substantial changes on the DNA persistence length upon binding, however, are much less common.

While SMFS was largely employed in the past to study DNA condensation induced by various compounds such as polyamines and proteins [12,14-17], the DNA complexes formed with Mitoxantrone (MTX) were never characterized at single molecule level. Here we report a SMFS characterization of this interaction using optical tweezers to stretch the DNA-MTX complexes in the entropic regime (forces < 10 pN). While higher forces (tens of pN) may bring information on the structure and structural transitions of these complexes, inside cells the DNA molecule is submitted to very small net forces, on the order of a few picoNewtons [18]. Therefore, to characterize the DNA-drug

* Corresponding author.
E-mail address: marcios.rocha@ufv.br (M.S. Rocha).

https://doi.org/10.1016/j.bbagen.2018.01.019
Received 27 November 2017; Received in revised form 17 January 2018; Accepted 30 January 2018
Available online 02 February 2018

interaction under conditions closer to that found inside living cells, which is important from the pharmacological point of view, here we employ forces as small as possible to perform the SMFS experiments.

MTX is currently used to treat various cancers such as acute myelogenous leukemia, breast cancer, non-Hodgkin's lymphoma, and others. Its cytotoxic effects consist of disrupting the DNA synthesis and repair, being also a topoisomerase II inhibitor. Concentrations below 1 μM are sufficient to inhibit cell growth by about 50% in vitro [19], which shows the efficiency of the drug in inhibiting cell proliferation. Here we show that, for these very low concentrations the drug behaves as a classical intercalator upon binding to the double-helix. For higher concentrations, however, it strongly condenses the DNA molecule, inducing a cooperative transition from the semi-flexible to the flexible regime of polymer elasticity. To the best of our knowledge, this is the first work that fully identifies and characterizes such kind of transition on the DNA elasticity caused by a small drug molecule, although MTX-induced DNA condensation was previously reported in bulk experiments [20]. In addition, the methodology developed here opens new possibilities in the investigation of the DNA condensation process and, more generally, in the investigation of phase transitions in polymer physics.

2. Materials and methods

The optical tweezers used here to perform the SMFS consist of a 1064 nm ytterbium-doped fiber laser operating in the TEM_{00} mode (IPG Photonics) mounted on a Nikon Ti-S inverted microscope with a 100× NA 1.4 objective.

Our samples consist of λ-DNA molecules (New England Biolabs) end-labeled with biotin in a Phosphate Buffered Saline (PBS) solution. One end of the DNA molecules is attached to a microscope coverslip surface, which is coated with streptavidin, while the other end is attached to a streptavidin-coated polystyrene bead with a diameter of 3 μm (Bangs Labs). In order to investigate the effects of the ionic strength on the DNA-MTX interaction, the measurements were carried under two different PBS buffers, whose compositions are detailed in Table 1.

MTX was purchased from Sigma-Aldrich (Cat. M6545) and used without further purification. The results reported below for the mechanical properties are averages over six FECs repeated for each drug concentration. All the error bars were calculated as the standard error of the mean from the six FECs. The experiments were carried out at room temperature (23°C). All additional details about the experimental methods and procedures can be found in ref. [21]. Fig. 1 shows the chemical structure of the MTX molecule.

3. Results and discussion

For simplicity, here we discuss separately the results obtained under the different ionic strengths. A comparison between the results obtained under these two conditions is then performed.

3.1. High ionic strength (I = 154 mM, [Na] = 150 mM)

Fig. 2 shows some typical FECs measured for the DNA-MTX complexes, obtained for MTX concentrations in the range $C_T \leqslant 7.5$ μM. For very small drug concentrations (*e.g.* 0.6 μM shown in Fig. 2), we measured a slight increase on the contour length. Nevertheless, as the drug concentration increases in the sample, the DNA molecule starts to condense. Such effect can be noted in the data of Fig. 2 from the strong decrease measured on the contour length of the DNA-MTX complexes as the drug concentration increases. This result corroborates with previous bulk studies which reported that MTX condenses the DNA molecule [20,22,23].

Table 1
Composition of the different PBS buffers used.

[Na] / Ionic strength	NaCl	Na_2HPO_4	NaH_2PO_4
150 mM/154 mM	140 mM	4.375 mM	1.25 mM
10 mM/14 mM	0	4.375 mM	1.25 mM

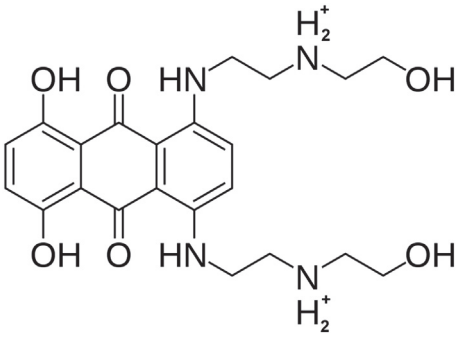

Fig. 1. Chemical structure of the MTX molecule.

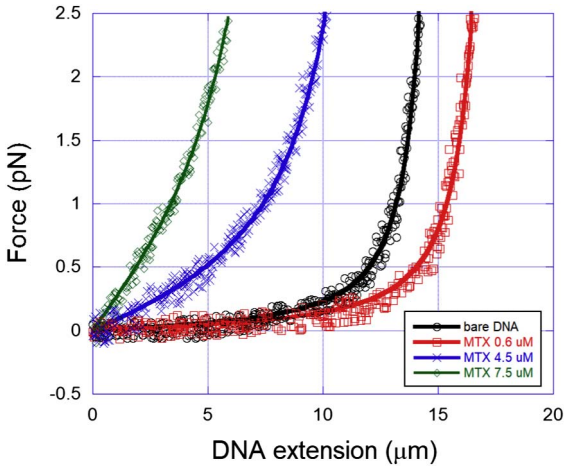

Fig. 2. *Points*: typical FECs measured for the DNA-MTX complexes at various drug concentrations, for the regime $C_T \leqslant 7.5$ μM. *Solid lines*: fittings to the Marko-Siggia WLC expression [7].

The WLC fittings were performed here using the Marko-Siggia expression for the entropic force [7] and are also shown in the figure as solid lines. These fittings could be performed only until a MTX concentration $C_T = 7.5$ μM, because for higher concentrations the FECs become straight lines, completely differing from the typical WLC behavior. Thus, for [Na] = 150 mM, the DNA-MTX complexes behave as semi-flexible polymers only at the concentration range $C_T \leqslant 7.5$ μM.

Fig. 3 shows more FECs, now obtained for higher MTX concentrations ($C_T > 7.5$ μM). As anticipated, the FECs are now straight lines and cannot be fitted to the WLC model. This result strongly indicates that the MTX-promoted DNA condensation process is correlated to a transition on the polymer elasticity regime. In other words, the DNA-MTX complexes become flexible polymers for $C_T > 7.5$ μM, allowing the condensation process.

In the theoretical framework, Halperin et al. [24] and Polotsky et al. [25] have predicted that the FEC of a completely condensed (totally collapsed) polymer should present three different regimes: (a) the force initially increases linearly with the extension, corresponding to the globule deformation; (b) the force then presents a plateau corresponding to the initiation of the unfolding process, *i.e.*, the change of the globular polymer into a linear one; and finally (c) the force increases again linearly with the extension when the polymer chain becomes linear. As can be seen in Fig. 3, we have not detected any force plateau in our experimental FECs: only the linear regime occurs here. This result is probably due to the fact that our DNA-MTX complexes are

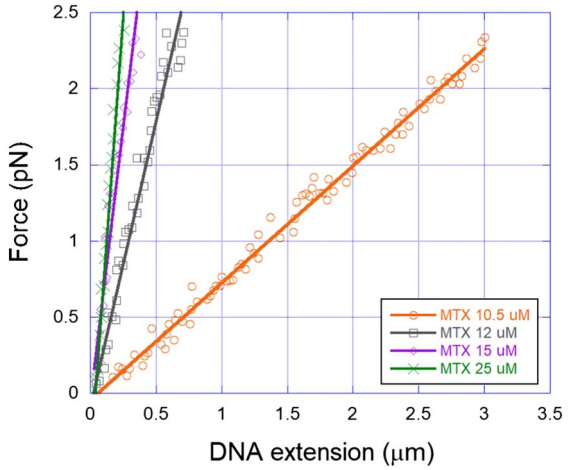

Fig. 3. *Points*: typical FECs measured for the DNA-MTX complexes at various drug concentrations, for the regime $C_T > 7.5\ \mu$M. *Solid lines*: fittings to the Gaussian chain (GC) model (Eq. (1)).

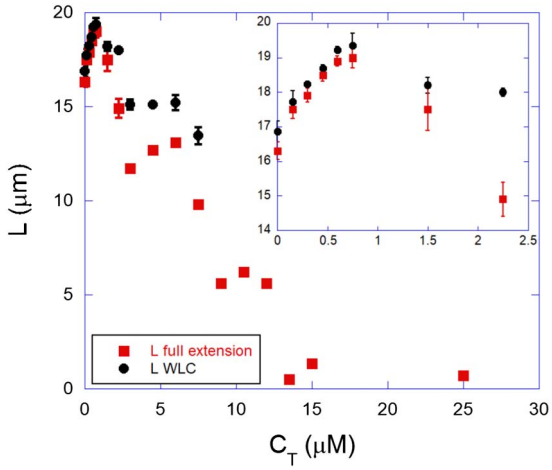

Fig. 4. Apparent contour length L of the DNA-MTX complexes as a function of MTX concentration in the sample C_T. We have determined the contour length by two different methods: from the WLC fitting (*black circles*) and by directly measuring the DNA full extension in the entropic regime, at a maximum stretching force of ~ 8 pN (*red squares*). *Inset*: a highlight of the data at low drug concentrations.

not completely collapsed. Thus, we were not able to see the force plateau predicted by those authors. In fact, experimentally it should be difficult to achieve such a condition. Experiments performed by various authors using traditional condensing agents such as polyamines, cobalt-hexamine and polyethylene-glycol have not presented yet this type of plateau in the FECs [12,16].

In their treatment, Polotsky et al. have shown that the unfolded condensates can be approximately described by an ideal (Gaussian) chain [25]. Thus we have used the Gaussian chain (GC) model, which is valid for flexible polymers [26], to fit the FECs (solid lines in Fig. 3). Such model predicts that the force F increases with the DNA extension z as

$$F = \frac{k_B T}{2R_g^2} z, \tag{1}$$

where k_B is Boltzmann's constant, T is the absolute temperature and R_g is the radius of gyration of the polymer chain.

Therefore, the radius of gyration of the flexible polymer chains can be directly determined from the linear fittings of Fig. 3. The concept of persistence length is not important in the context of the GC model, since the polymer chain is very flexible and there is no energetic cost to introduce bendings in the polymer chain. The apparent contour length, on the other hand, can be obtained directly from the stretching experiments by measuring the DNA full extension in the entropic regime. Here we have performed such measurements for each MTX concentration at a force of ~ 8 pN, *i.e.*, close to the limit of the entropic force regime, in order to guarantee that values obtained for the contour length do not have enthalpic contributions.

The complete behavior of the DNA-MTX contour length discussed above is evidenced in Fig. 4, in which we show the values obtained for such mechanical property at various MTX concentrations. We have determined the contour length by two different methods: from the WLC fitting (*black circles*) and by direct measuring the DNA full extension in the entropic regime, at a maximum stretching force of ~ 8 pN (*red squares*), as mentioned before. This second method has the advantage to be a model-free measurement. The purpose of using these two different methodologies to measure the same quantity is to explicitly show that the contour length results obtained from the WLC fittings start to loose accuracy when the DNA condensation begins, at $C_T \gtrsim 1.5\ \mu$M. Such conclusion is evidenced in the inset of Fig. 4, which highlights the regime of low drug concentrations.

Observe that the contour length of the DNA-MTX complexes initially increases for $C_T \lesssim 0.75\ \mu$M. Such increase is very similar to that found in intercalative binding [27], and thus allows one to assume that MTX behaves as a typical intercalator at very low drug concentrations. Such assumption will be confirmed later by determining the MTX binding parameters at this concentration range. Observe also that the values obtained for the contour length with the two different methodologies agree within the error bars at this concentration range ($C_T \lesssim 0.75\ \mu$M). Such result is expected, since the changes on the mechanical properties of DNA introduced by intercalating molecules are in general only slight [27,28]. Therefore, the DNA-MTX complexes still behave as semi-flexible polymers for $C_T \lesssim 0.75\ \mu$M and the WLC model works well for determining the contour length, returning results that agree with the model-free measurements. For $C_T \gtrsim 1.5\ \mu$M, on the other hand, the contour length starts to decrease because the condensation process starts, and the values returned from the WLC fittings begin to deviate from those obtained by the model-free measurements.

In Fig. 5 we show the behavior of the persistence length obtained from the WLC fittings for the same DNA-MTX complexes. Observe that such parameter firstly increases for very small MTX concentrations ($C_T \lesssim 0.6\ \mu$M), but strongly decreases for higher concentrations. Again, this initial increase is typical of intercalative binding [27,28], corroborating with the assumption drawn from the contour length data about the binding mode at very low MTX concentrations. For $C_T \gtrsim 2.25\ \mu$M, on the

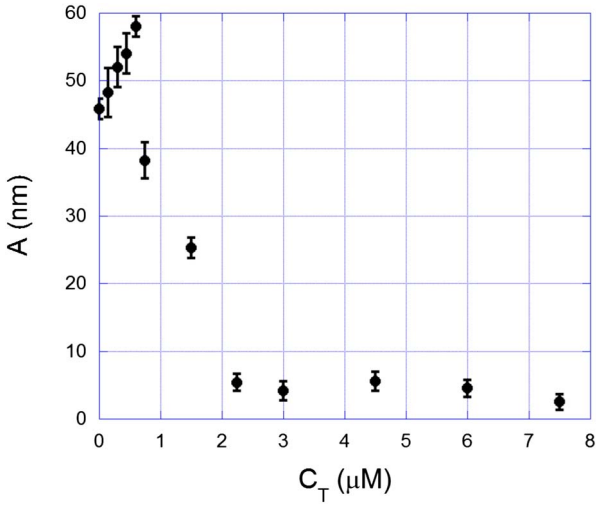

Fig. 5. Persistence length A of the DNA-MTX complexes as a function of MTX concentration in the sample C_T.

other hand, the values obtained for the persistence length are considerably small (< 10 nm), showing that the flexibility of the DNA-MTX complexes has highly increased. The fact that the FECs approach their shape to straight lines as the MTX concentration increases (see Figs. 2 and 3) strengthens such interpretation.

The results discussed until now allow one to identify distinct regimes of drug concentration with different mechanical behaviors of the DNA-MTX complexes. At low drug concentrations ($C_T \lesssim 0.75\ \mu$M), MTX behaves as a typical intercalator when interacting with DNA, increasing both the contour and persistence lengths of the molecule upon binding. For higher concentrations, otherwise, MTX-induced DNA condensation starts to take place, with a strong decrease on both mechanical properties. During the condensation process, we have explicitly shown that the flexibility of the DNA-MTX complexes suffers a transition from the semi-flexible to the flexible regime, and the FECs become straight lines for $C_T > 7.5\ \mu$M.

MTX is a divalent (+2) cationic molecule in pH 7.4 [23,29] and has a relatively large size (see Fig. 1). Therefore, in principle one should not expect that it can condense DNA, a feature mostly observed for molecules with charge equal or higher than +3 [30,31]. Nevertheless, DNA condensation still occurs here, probably because the position of the bound MTX molecules is approximately fixed along the double-helix at the intercalation sites. Thus, there is a considerable positional correlation of the positive charges, a feature necessary for the condensation process [32–34]. Another possibility is MTX self-association forming dimers or aggregates of higher order, a feature common for most anthracyclines [21,23,35,36]. Such self-association in practice increases the effective charge of the ligand, making DNA condensation possible.

To advance further in the characterization of the condensation process, we use the radius of gyration of the complexes in order to connect the different mechanical behaviors obtained in the two flexibility regimes. For $C_T > 7.5\ \mu$M, the radius of gyration R_g was determined directly from the fittings of the FECs to Eq. (1), since they are straight lines at this concentration range, as explained before. For $C_T \leqslant 7.5\ \mu$M, the radius of gyration was calculated from the persistence and contour lengths as

$$R_g = \sqrt{\frac{1}{3}AL\left(1 - \frac{3A}{L} + \ldots\right)}. \tag{2}$$

The behavior R_g as a function of the MTX concentration C_T is shown in Fig. 6. Three different regimes can be promptly identified: (a) For $C_T \leqslant 0.6\ \mu$M the radius of gyration increases as a function of the MTX concentration, indicating that the intercalative mechanism is strongly dominant here; (b) For $0.6\ \mu\text{M} \leqslant C_T \leqslant 2.25\ \mu$M, an abrupt and irregular decrease of the radius of gyration occurs, indicating a transition to the condensation regime; and finally (c) For $C_T \geqslant 2.25\ \mu$M, a regular sigmoidal decrease of the radius of gyration as a function of C_T occurs. This behavior indicates that the regular condensation process starts at $C_T \sim 2.25\ \mu$M, a result compatible to that shown in Fig. 4.

In addition, observe that for $C_T \leqslant 7.5\ \mu$M, we show two different results calculated using the values of the contour length from the WLC fittings (*black circles*) as well as from the full extension measurements (*red squares*). For $C_T > 7.5\ \mu$M, on the other hand, there is only one result, obtained from the FECs fittings to the GC model (Eq. (1)). In any case, observe that after the condensation starts, R_g monotonically decreases as a function of the MTX concentration, as expected.

The behavior of R_g can be modeled in order to allow quantitative insights on the MTX-induced condensation process. To perform such a task, we concentrate our attention on the regular sigmoidal decrease of this parameter (part (c) of Fig. 6). Part (b) (abrupt and irregular decrease) is probably much more complicated to be modeled since it is a transition between two very distinct regimes. Due to its pronounced sigmoidal behavior, here we propose that the radius of gyration should decrease as a function of the bound MTX molecules as a Hill-type process, *i.e.*,

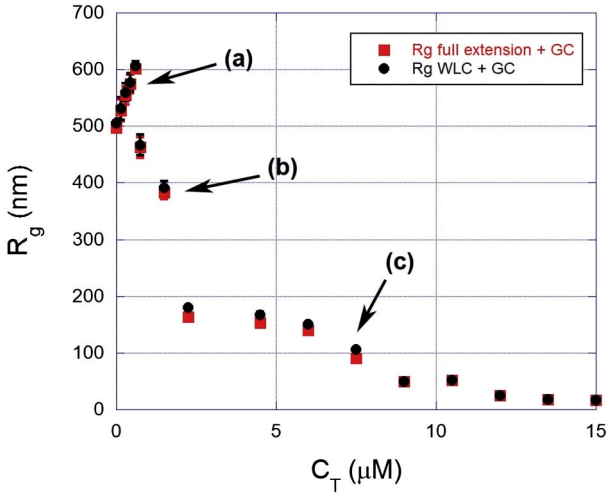

Fig. 6. Radius of gyration R_g as a function of the MTX concentration C_T. For $C_T \leqslant 7.5\ \mu$M, we show two different results calculated using the values of the contour length from the WLC fittings (*black circles*) as well as from the full extension measurements (*red squares*). For $C_T > 7.5\ \mu$M, on the other hand, there is only one result, obtained from the FECs fittings to the GC model (Eq. (1)). Three distinct regimes can be noted: (a) For $C_T \leqslant 0.6\ \mu$M the radius of gyration increases; (b) For $0.6\ \mu\text{M} \leqslant C_T \leqslant 2.25\ \mu$M, an abrupt and irregular decrease occurs; and finally (c) For $C_T \geqslant 2.25\ \mu$M, a final regular sigmoidal decrease occurs.

$$R_g = R_g^0\left(1 - \frac{r^n}{r_c^n + r^n}\right), \tag{3}$$

where R_g^0 is the initial value of the radius of gyration (in this regime), r is the bound drug concentration (C_b) normalized by the number of available binding sites (DNA base-pairs, C_{bp}), r_c is a characteristic value of r, and n is the Hill exponent. The Hill exponent n measures the cooperative degree of a given biochemical process. If $n > 1$, the process is positively cooperative, *i.e.*, a bound ligand molecule facilitates the occurrence of the process. If $n < 1$, otherwise, the process is negatively cooperative and a bound ligand molecule makes difficult the occurrence of the process. If $n = 1$, the process is non-cooperative and thus independent of the number of bound ligand molecules.

In principle, other sigmoidal functions could be used to fit the experimental data and maybe should work well. Nevertheless, the proposed Hill-type function is convenient here because of the biochemical interpretation of the Hill coefficient discussed above, which gives us an estimation of the cooperativity of the MTX-induced DNA condensation process. Previous bulk studies have provided evidence that MTX binds cooperatively to the double-helix [22,23,37,38], but here we are in a position to quantify the degree of cooperativity at single molecule level.

In order to fit the experimental data of Fig. 6 with Eq. (3), one must find the relationship between the bound drug fraction $r = C_b/C_{bp}$ and the total drug concentration used in the sample C_T. Observe that $C_T = C_b + C_f$, where C_f is the free (not bound) drug concentration in the sample. These quantities can be related by a convenient binding isotherm that captures the physical chemistry of the interaction. Since MTX intercalates the double-helix, the most convenient binding isotherm to be used is the McGhee - von Hippel neighbor exclusion model (NEM) [39]. This model describes very well the binding of intercalating molecules to the DNA and can be used to fit the contour length data of Fig. 4 for $C_T \leqslant 0.75\ \mu$M (the concentration range in which the contour length increases, *i.e.*, in which the intercalative behavior manifests).

In Fig. 7 we show the behavior of the normalized contour length $\Theta = (L - L_0)/L_0$ as a function of the MTX concentration C_T for the range $C_T \leqslant 0.75\ \mu$M. For convenience to fit with the NEM binding isotherm, the axis was interchanged. The fitting is shown as a dashed line in Fig. 7 and was performed using the procedure detailed described in ref. [1], using the equation

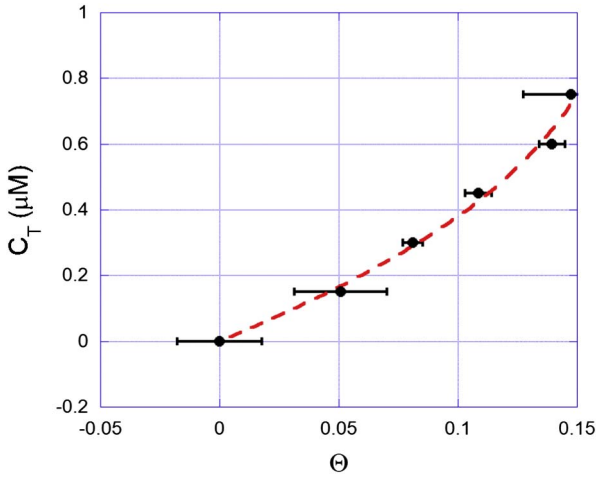

Fig. 7. Behavior of the normalized contour length $\Theta = (L\,L_0)/L_0$ as a function of the MTX concentration C_T for the range $C_T \leqslant 0.75\ \mu$M.

$$C_T = \frac{C_{bp}}{\gamma}\Theta + \frac{\Theta(\gamma - N\Theta + \Theta)^{N-1}}{K(\gamma - N\Theta)^N}. \quad (4)$$

In this model, N is the exclusion parameter (binding site size), K is the association equilibrium constant and γ is the ratio between the extension elongated per bound ligand and the distance between two consecutive base-pairs ($\sim$ 0.34 nm for B-DNA). For typical intercalators, $\gamma \sim 1$ [4,40]. In ref. [1,27] it was shown that $\Theta = \gamma r \sim r$ for the typical increase on the contour length induced by intercalators. By fitting the experimental data of Fig. 7 to Eq. (4) with $\gamma = 1$ fixed, we obtain the binding parameters $N = 3.5 \pm 0.5$ and $K = (1.6 \pm 0.4) \times 10^6\ \mathrm{M}^{-1}$. Both parameters are on the same order of magnitude of the results found for typical intercalators [4,21,27,41,42] and also corroborate to results obtained from bulk measurements for the DNA-MTX complexes [23,37,38]. The value of N indicates that each MTX molecule occupies 3 to 4 base pairs upon intercalation. The order of magnitude of the association constant ($10^6\ \mathrm{M}^{-1}$), on the other hand, indicates that MTX binds strongly to the double-helix, with a value of K higher than other classic anthracycline drugs such as daunomycin and doxorubicin [21,27].

Once the binding parameters (and consequently the binding isotherm) for the DNA-MTX system were determined, one promptly knows the value of $r \sim \Theta$ for each value of C_T. Assuming that the bound site fraction r does not change upon the condensation process, we can replot the data of R_g from Fig. 6 as a function of r in order to fit with the proposed model (Eq. (3)). Fig. 8 shows the experimental data along with the fitting with Eq. (3) (*dashed line*), for the concentration range corresponding to the sigmoidal decrease (part (c) of Fig. 6), as discussed above. Observe that the proposed model fits well to the experimental data, and from such fitting we determine the Hill exponent n, and also the characteristic constants R_g^0 and r_c.

In Table 2 we show the results obtained from the fittings. Observe that the two different data sets have the same parameters within the error bars, which indicates that the error introduced by using the WLC model to determine the contour lengths at the beginning of the condensation process is not much relevant to the present analysis. The values obtained for R_g^0 and r_c are characteristics of the curves shown in Fig. 8, as mentioned before. The high value found for the Hill exponent ($n > > 1$), on the other hand, indicates that the MTX-induced condensation process is strongly cooperative. In other words, the transition from the semi-flexible to the flexible regime of polymer elasticity is highly cooperative, occurring more easily as the MTX concentration is increased. A similar conclusion was previously achieved by Teif, studying the DNA condensation process induced by the polyamine spermidine [43]. In this reference, Teif has argued that the positive cooperativity verified in the DNA condensation process is due to the

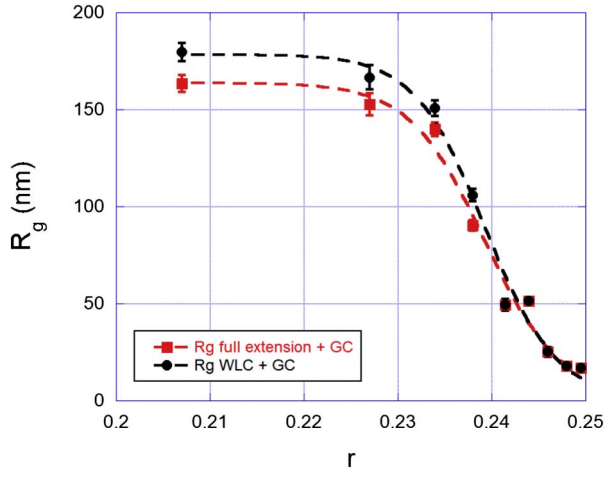

Fig. 8. Radius of gyration R_g as a function of the bound drug fraction r. *Dashed lines* are fittings to the proposed model (Eq. (3)).

Table 2
Parameters of the two R_g data of Fig. 8 ([Na] = 150 mM).

R_g data	n	R_g^0 (nm)	r_c
full ext. + GC	59 ± 7	164 ± 7	0.239 ± 0.001
WLC + GC	63 ± 7	178 ± 7	0.239 ± 0.001

positional correlation of the bound ligands, which induces attractive forces between the various different DNA segments [43]. A recent review on this subject can be found in ref. [44].

3.2. Low ionic strength (*I* = 14 mM, [Na] = 10 mM)

In Fig. 9 we show some typical FECs measured for the DNA-MTX complexes at the low ionic strength condition. Observe that the qualitative behavior is the same one observed at high ionic strengths: for low drug concentrations (in this case $C_T \leqslant 3\ \mu$M), the FECs present the usual WLC shape, indicating that the DNA-MTX complexes are still semi-flexible polymers at this concentration range. For higher drug concentrations (*e.g.* 4.5 μM shown in the figure), the FECs become straight lines, indicating that the DNA-MTX complexes also become flexible polymers here. The *solid lines* in Fig. 9 are fittings to the WLC (bare DNA

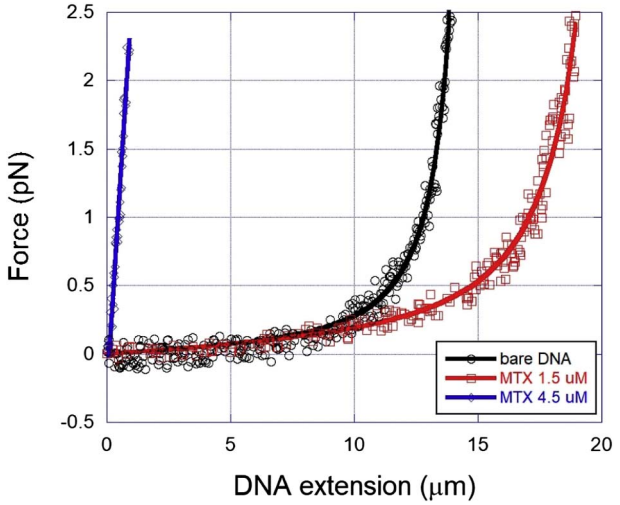

Fig. 9. *Points*: typical FECs measured for the DNA-MTX complexes at some drug concentrations, for [Na] = 10 mM. *Solid lines*: fittings to the WLC (bare DNA and 1.5 μM) or GC (4.5 μM) models.

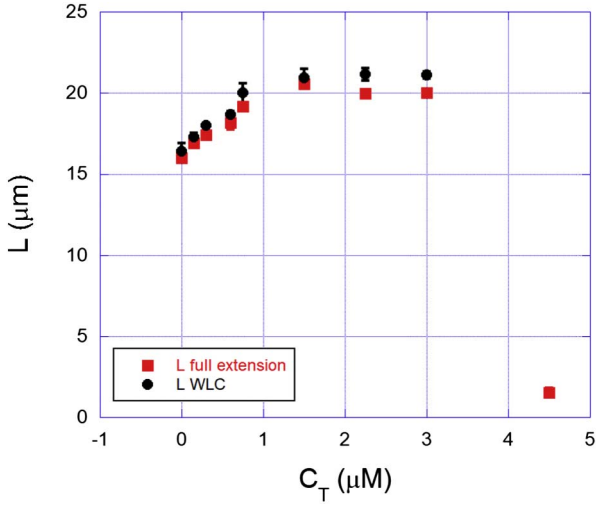

Fig. 10. Contour length L of the DNA-MTX complexes as a function of MTX concentration in the sample C_T, for [Na] = 10 mM.

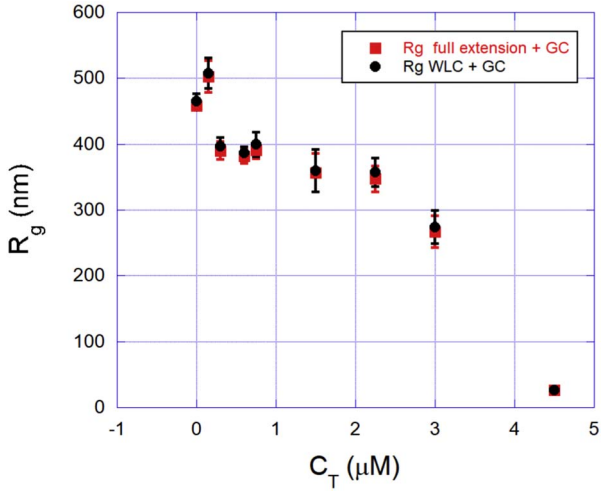

Fig. 12. Radius of gyration R_g as a function of the MTX concentration C_T, for [Na] = 10 mM.

and 1.5 μM) or GC (4.5 μM) models. One should observe that the FEC regime change occurs at a considerably lower concentration ($\sim$ 3 μM) for [Na] = 10 mM when compared to the former situation ($\sim$ 7.5 μM for [Na] = 150 mM). This result is a first indication that the ionic strength plays an important role in this process, as expected for a divalent cationic drug like MTX.

In Fig. 10 we show the contour length of the DNA-MTX complexes obtained for [Na] = 10 mM. Observe again that the qualitative behavior is similar to the former case ([Na] = 150 mM): the contour length initially increases until $C_T \sim 3$ μM, and then decreases when the DNA condensation starts. For [Na] = 10 mM, however, such decrease is much more abrupt. In fact, we were not able to obtain more data points for $C_T > 4.5$ μM due to the strong DNA condensation induced by MTX at such condition. Here we have again measured the contour length by two independent methods (WLC fitting and by measuring the DNA full extension). In the semi-flexible regime, where the WLC model works well ($C_T \leqslant 3$ μM), the results are very similar.

In Fig. 11, on the other hand, we show the persistence length data obtained for [Na] = 10 mM. Again, the qualitative behavior is the same: it initially increases for low drug concentrations, and then strongly decreases.

In Fig. 12 we show the radius of gyration as a function of the drug concentration in the sample, for [Na] = 10 mM. Such mechanical parameter was determined using exactly the same procedure described in the former case ([Na] = 150 mM). Here, again, the curve presents three distinct regimes: (a) an initial increase for very low concentrations ($C_T \leqslant$ 0.15 μM), where the intercalative behavior of the drug dominates; (b) an abrupt decrease that indicates the transition to the condensation regime; and finally, (c) a regular sigmoidal decrease of the radius of gyration for $C_T \geqslant$ 0.3 μM.

Such result confirms that the ionic strength plays a fundamental role in the condensation process. In fact, the transition from regime (a) to (c) occurs at concentration range of $\sim$ 0.6 to 1.5 μM for [Na] = 150 mM and of $\sim$ 0.15 to 0.30 μM for [Na] = 10 mM. Thus, the MTX-induced condensation process is facilitated at low ionic strengths, occurring at lower drug concentrations. In addition, for [Na] = 10 mM the transition concentration range is narrower, indicating that the transition from regimes (a) to (c) occurs more abruptly.

In order to advance in our analysis, in Fig. 13 we show the behavior of the normalized contour length $\Theta = (L - L_0)/L_0$ as a function of the MTX concentration C_T for the range $C_T \leqslant 3$ μM (the range in which the intercalative behavior dominates). The *dashed line* is a fitting to Eq. (4), performed using the same procedure of the former case. From the fitting we extract the binding parameters $N = 2.9 \pm 0.2$ and $K = (6 \pm 1) \times 10^6$ M^{-1}. These parameters are again on the order of magnitude expected for intercalators. Observe that the binding site size N is the same of the former case within the error bars. The binding constant, on the

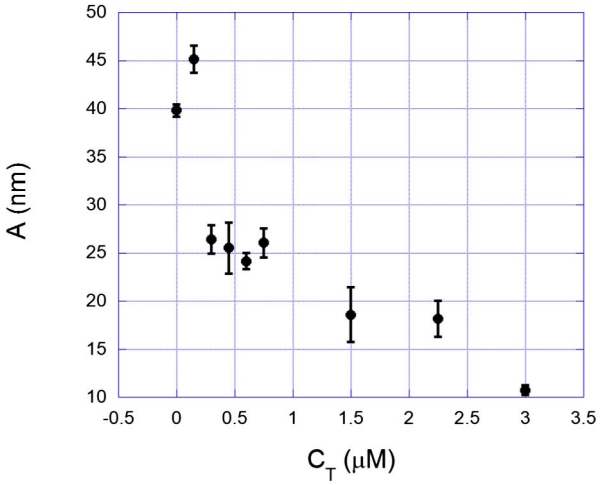

Fig. 11. Persistence length A of the DNA-MTX complexes as a function of MTX concentration in the sample C_T, for [Na] = 10 mM.

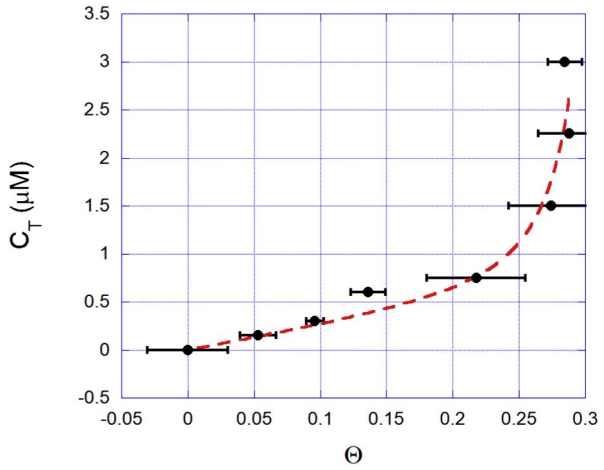

Fig. 13. Behavior of the normalized contour length $\Theta = (L - L_0)/L_0$ as a function of the MTX concentration C_T for [Na] = 10 mM.

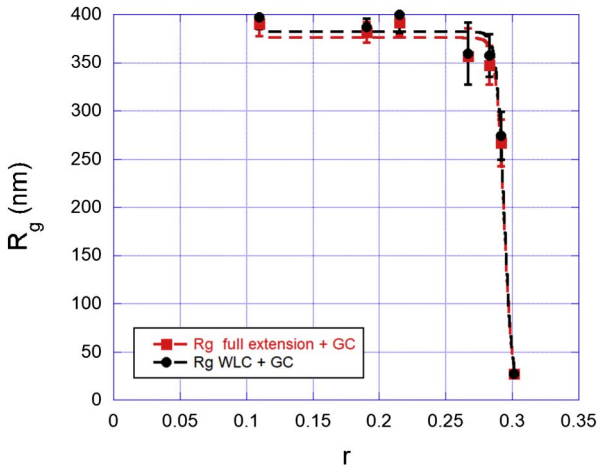

Fig. 14. Radius of gyration R_g as a function of the bound drug fraction r for [Na] = 10 mM. *Dashed lines* are fittings to the proposed model (Eq. (3)).

Table 3
Parameters of the two R_g data of Fig. 14 ([Na] = 10 mM).

R_g data	n	R_g^0 (nm)	r_c
full ext. + GC	95 ± 18	376 ± 8	0.294 ± 0.001
WLC + GC	98 ± 20	382 ± 9	0.294 ± 0.001

other hand, has increased ~ 3.75×. Such result again evidences the important role of the ionic strength on the present system: the strong electrostatic interactions between the positively charged drug molecules and the negative phosphate backbone of the DNA double-helix is more screened as more counterions are present in solution, *i.e.*, at higher ionic strengths.

In Fig. 14 we show the radius of gyration R_g as a function of the bound site fraction r obtained for [Na] = 10 mM using the same procedure described before for the high ionic strength case. The main difference from the former case is that here R_g decreases much more abruptly as a function of r, which indicates a significant increase on the cooperativity degree of the process. In fact, in Table 3 we show the parameters obtained from the two fittings shown in Fig. 14. Observe that the Hill exponent n has considerably increased in relation to the former result, indicating that the process has become more cooperative.

Nevertheless, a critical analysis of the fitting processes shown in Figs. 8 and 14 must be performed here. Observe that the proposed model used to fit the experimental data, Eq. (3), is the simplest one possible, such that the Hill exponents returned from the fittings are only indicative of the cooperativity degree and should not be taken as exact numbers. In any case, observe that this parameter measures the sharpness of the R_g decrease. For a decay represented by step function, for example, one has $n \to \infty$. Therefore, the results presented here confirm that the DNA condensation process induced by the divalent drug MTX is strongly cooperative, and such cooperativity increases for lower ionic strengths.

At single molecule level, the condensation process is in general recognized as an "all-or-none" folding transition [44], compatible with a R_g decrease well represented by a step function which reflects the high cooperativity of such process. The behavior of R_g obtained in Figs. 8 and 14 is compatible to this result, specially at low ionic strengths (Fig. 14) where the relevant electrostatic interactions responsible for the condensation process are less screened.

4. Conclusions

The present work reports a cooperative transition from the semi-flexible to the flexible regime of polymer elasticity during the condensation of the DNA molecule induced by the drug MTX. By using SMFS, we show that the FECs of the DNA-MTX complexes deviates from the typical WLC behavior as the drug concentration in the sample increases, becoming straight lines for sufficiently high concentrations. For the regular condensation process, the radius of gyration of the complexes decreases monotonically as a function of the MTX concentration, and the curve presents a sigmoidal shape, from which we extract some important parameters that characterize the interaction; in particular, the degree of cooperativity. We show that this parameter increases for lower ionic strengths, where the relevant electrostatic interactions between DNA and MTX are less screened. The present methodology can be promptly applied to other ligands that condense the DNA molecule, opening new possibilities in the investigation of this type of process and, more generally, in the investigation of phase transitions in polymer physics.

Transparency document

The Transparency document associated with this article can be found, in online version.

Acknowledgments

This work was supported by the Brazilian agencies: Fundação de Amparo à Pesquisa do Estado de Minas Gerais (FAPEMIG), Conselho Nacional de Desenvolvimento Científico e Tecnológico (CNPq) and Coordenação de Aperfeiçoamento de Pessoal de Nível Superior (CAPES). The authors thank Esio B. Ramos for the helpful discussions and suggestions.

References

[1] M.S. Rocha, Extracting physical chemistry from mechanics: a new approach to investigate DNA interactions with drugs and proteins in single molecule experiments, Integr. Biol. 7 (2015) 967–986.
[2] M.J. McCauley, M.C. Williams, Mechanisms of DNA binding determined in optical tweezers experiments, Biopolymers 85 (2007) 154–168.
[3] M.J. McCauley, M.C. Williams, Optical tweezers experiments resolve distinct modes of DNA-protein binding, Biopolymers 91 (2009) 265–282.
[4] A. Sischka, K. Tönsing, R. Eckel, S.D. Wilking, N. Sewald, R. Rios, D. Anselmetti, Molecular mechanisms and kinetics between DNA and DNA binding ligands, Biophys. J. 88 (2005) 404–411.
[5] J.-F. Allemand, D. Bensimon, V. Croquette, Stretching DNA and RNA to probe their interactions with proteins, Curr. Opin. Struc. Biol. 13 (2003) 266–274.
[6] R. Krautbauer, L.H. Pope, T.E. Schrader, S. Allen, H.E. Gaub, Discriminating small molecule DNA binding modes by single molecule force spectroscopy, FEBS Lett. 510 (2002) 154–158.
[7] J.F. Marko, E.D. Siggia, Stretching DNA, Macromolecules 28 (1995) 8759–8770.
[8] S.B. Smith, L. Finzi, C. Bustamante, Direct mechanical measurements of the elasticity of single DNA molecules by using magnetic beads, Science 258 (1992) 1122–1126.
[9] T. Odjik, Stiff chains and filaments under tension, Macromolecules 28 (1995) 7016–7018.
[10] C. Bustamante, J.F. Marko, E.D. Siggia, S. Smith, Entropic elasticity of lambda-phage DNA, Science 265 (1994) 1599–1600.
[11] M.D. Wang, H. Yin, R. Landick, J. Gelles, S.M. Block, Stretching DNA with optical tweezers, Biophys. J. 72 (1997) 1335–1346.
[12] C.G. Baumann, V.A. Bloomfield, S.B. Smith, C. Bustamante, M.D. Wang, S.M. Block, Stretching of single collapsed DNA molecules, Biophys. J. 78 (2000) 1965–1978.
[13] C.G. Baumann, S.B. Smith, V.A. Bloomfield, C. Bustamante, Ionic effects on the elasticity of single DNA molecules, Proc. Natl. Acad. Sci. U. S. A. 94 (1997) 6185–6190.
[14] Y. Cui, C. Bustamante, Pulling a single chromatin fiber reveals the forces that maintain its higher-order structure, Proc. Natl. Acad. Sci. U. S. A. 97 (2001) 127–132.
[15] M.L. Bennink, S.H. Leuba, G.H. Leno, J. Zlatanova, B.G. de Grooth, J. Greve, Unfolding individual nucleosomes by stretching single chromatin fibers with optical tweezers, Nat. Struct. Biol. 8 (2001) 606–610.
[16] M.S. Rocha, A.G. Cavalcante, R. Silva, E.B. Ramos, On the effects of intercalators in DNA condensation: a force spectroscopy and gel electrophoresis study, J. Phys. Chem. B 118 (2014) 4832–4839.
[17] C.H.M. Lima, M.S. Rocha, E.B. Ramos, Unfolding DNA condensates produced by DNA-like charged depletants: a force spectroscopy study, J. Chem. Phys. 146 (2017) 054901.
[18] R. Blossey, H. Schiessel, The dynamics of the nucleossome: thermal effects,

external forces and ATP, FEBS J. 278 (2011) 3619–3632.
[19] F. Traganos, B. Kaminska-Eddy, Z. Darzynkiewicz, Caffeine reverses the cytotoxic and cell kinetic effects of Novantrone (mitoxantrone), Cell prolif. 24 (1991) 305–319.
[20] J. Kapuscinski, Z. Darzynkiewicz, Condensation of nucleic acids by intercalating aromatic cations, Proc. Natl. Acad. Sci. U. S. A. 81 (1984) 7368–7372.
[21] E.F. Silva, R.F. Bazoni, E.B. Ramos, M.S. Rocha, DNA-doxorubicin interaction: new insights and peculiarities, Biopolymers 107 (2017) e22998.
[22] J. Kapuscinski, Z. Darzynkiewicz, Relationship between the pharmacological activity of antitumor drugs Ametantrone and mitoxantrone (Novatrone) and their ability to condense nucleic acids, Proc. Natl. Acad. Sci. U. S. A. 83 (1986) 6302–6306.
[23] L.S. Rosenberg, M.J. Carvlin, T.R. Krugh, The antitumor agent Mitoxantrone binds cooperatively to DNA: evidence for heterogeneity in DNA conformation, Biochemistry 25 (1986) 1002–1008.
[24] A. Halperin, E.B. Zhulina, On the deformation behaviour of collapsed polymers, Europhys. Lett. 15 (1991) 417–421.
[25] A.A. Polotsky, M. Daoud, O.V. Borisov, T.M. Birshtein, A quantitative theory of mechanical unfolding of a homopolymer globule, Macromolecules 43 (2010) 1629–1643.
[26] I. Teraoka, Polymer Solutions: An Introduction to Physical Properties, John Wiley and Sons Inc., 2002.
[27] M.S. Rocha, M.C. Ferreira, O.N. Mesquita, Transition on the entropic elasticity of DNA induced by intercalating molecules, J. Chem. Phys. 127 (2007) 105108.
[28] R.F. Bazoni, C.H.M. Lima, E.B. Ramos, M.S. Rocha, Force-dependent persistence length of DNA-intercalator complexes measured in single molecule stretching experiments, Soft Matt. 11 (2015) 4306–4314.
[29] M. Enache, A.M. Toader, M.I. Enache, Mitoxantrone-surfactant interactions: a physicochemical overview, Molecules 21 (2016) 1356.
[30] V.A. Bloomfield, Condensation of DNA by multivalent cations: considerations on mechanism, Biopolymers 31 (1991) 1471–1481.
[31] V.A. Bloomfield, DNA Condensation by multivalent cations, Biopolymers 44 (1997) 269–282.
[32] N. Grønbech-Jensen, R.J. Mashl, R.F. Bruinsma, W.M. Gelbart, Counterion-induced attraction between rigid polyelectrolytes, Phys. Rev. Lett. 78 (1997) 2477–2480.
[33] R.G. Winkler, M. Gold, P. Reineker, Collapse of polyelectrolyte macromolecules by counterion condensation and ion pair formation: a molecular dynamics simulation study, Phys. Rev. Lett. 80 (1998) 3731–3734.
[34] M. Khan, B. Jönsson, Electrostatic correlations fold DNA, Biopolymers 49 (1999) 121–125.
[35] J.B. Chaires, N. Dattagupta, D.M. Crothers, Self-association of danomycin, Biochemistry 21 (1982) 3927–3932.
[36] C. Pérez-Arnaiz, N. Busto, J.M. Leal, B. García, New insights into the mechanism of the DNA/Doxorubicin interaction, J. Phys. Chem. B 118 (2014) 1288–1295.
[37] J. Kapuscinski, Z. Darzynkiewicz, F. Traganos, M.R. Melamed, Interactions of a new antitumor agent, 1,4-dihydroxy-5,8-bis[[2-[(2-hydroxyethyl)amino]-ethyl] amino]-9,10-anthracenedione, with nucleic acids, Biochem. Pharmacol. 30 (1981) 231–240.
[38] Z. Hajihassan, A. Rabbani-Chadegani, Studies on the binding affinity of anticancer drug mitoxantrone to chromatin, DNA and histone proteins, J. Biomed. Sci. 16 (2009) 31.
[39] J.D. McGhee, P.H. von Hippel, Theoretical aspects of DNA-protein interactions - cooperative and non-cooperative binding of large ligands to a one-dimensional homogeneous lattice, J. Mol. Biol. 86 (1974) 469–489.
[40] H. Fritzsche, H. Triebel, J.B. Chaires, N. Dattagupta, D.M. Crothers, Studies on interaction of anthracycline antibiotics and deoxyribonucleic-acid: geometry of intercalation of Iremycin and Daunomycin, Biochemistry 21 (1982) 3940–3946.
[41] J.B. Chaires, N. Dattagupta, D.M. Crothers, Studies on interaction of anthracycline antibiotics and deoxyribonucleic-acid - equilibrium binding-studies on interaction of Daunomycin with deoxyribonucleic-acid, Biochemistry 21 (1982) 3933–3940.
[42] B. Gaugain, J. Barbet, N. Capelle, B.P. Roques, J.L. Pecq, DNA bifunctional intercalators .2. Fluorescence properties and DNA binding interaction of an ethidium homodimer and an acridine ethidium heterodimer, Biochemistry 17 (1978) 5078–5088.
[43] V.B. Teif, Ligand-induced DNA condensation: choosing the model, Biophys. J. 89 (2005) 2574–2587.
[44] A.F. Jorge, S.C.C. Nunes, T.F.G.G. Cova, A.A.C.C. Pais, Cooperative action in DNA condensation, Curr. Opin. Coll. Int. Sci. 26 (2016) 66–74.